

Deconvolutional Density Network: Free-Form Conditional Density Estimation

Bing Chen^{1, #}, Mazharul Islam^{1, #}, Lin Wang^{1, *}, Jisuo Gao¹, and Jeff Orchard²

¹Shandong Provincial Key Laboratory of Network Based Intelligent Computing,
University of Jinan, Jinan 250022, China

²Cheriton School of Computer Science,
University of Waterloo, Waterloo, Ontario N2L 3G1, Canada

Abstract

Conditional density estimation is the task of estimating the probability of an event, conditioned on some inputs. A neural network can be used to compute the output distribution explicitly. For such a task, there are many ways to represent a continuous-domain distribution using the output of a neural network, but each comes with its own limitations for what distributions it can accurately render. If the family of functions is too restrictive, it will not be appropriate for many datasets. In this paper, we demonstrate the benefits of modeling free-form distributions using deconvolution. It has the advantage of being flexible, but also takes advantage of the topological smoothness offered by the deconvolution layers. We compare our method to a number of other density-estimation approaches, and show that our Deconvolutional Density Network (DDN) outperforms the competing methods on many artificial and real tasks, without committing to a restrictive parametric model.

1 Introduction

Machine learning is used in a variety of supervised learning situations, for which both the inputs and desired outputs are specified. Learned models can map inputs to a discrete set of labels (e.g. *classifying* handwritten digits), or to values in a continuous domain (e.g. *regressing* temperature).

Conditional Density Estimation (CDE) is a more general learning task, where the goal is to return the *distribution* over a range of output values. More precisely, given an input x , estimate $p(y|x)$, where $y \in \mathcal{D}$. For example, consider a dataset with inputs consisting of people's age and gender, and we wish to estimate their weights. Not just the person's weight, but the distribution over all possible weights. Figure 1 illustrates this example, showing the body-weight distributions for 3 different age/gender combinations. Notice that the distributions can change markedly, depending on the inputs.

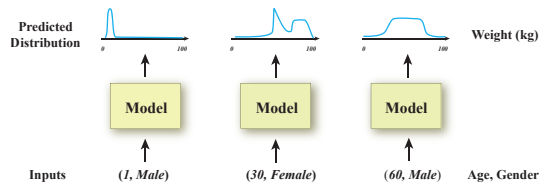


Figure 1: Example Conditional Density Estimation, estimating the distribution over different weights.

Both authors contributed equally to this work

* Corresponding author: Lin Wang <wangplanet@gmail.com>

Both classification and regression can be posed as instances of CDE; the location of the maximum (mode) corresponds to the output class, and the mean of the distribution could be used as the output for regression. But these do not tell the whole story, and often the full distribution is much preferred, especially in cases when the distributions are broad or multi-modal. Such uncertainty in the output can arise from a number of different sources: stochasticity in the underlying phenomenon, incomplete training data, or insufficient capacity in our model (even if the underlying phenomenon is deterministic).

One problem with CDE is that continuous-domain functions, such as probability density functions (PDFs), are infinite-dimensional; in theory, an infinite number of parameters is needed to specify an arbitrary function. This is not practically possible, and is further exacerbated by the finite size of datasets used to tune the parameters.

The only option is to limit ourselves to a finite-dimensional subspace for our output functions. For example, the model could learn to output the mean and standard deviation of a Gaussian distribution. Or, our model could output a number of such pairs, constructing a PDF as a Gaussian mixture model [1, 2].

Hence, we need to apply some assumptions to our model, so-called *inductive biases*. Naturally, it is helpful if one knows the general form of the target distribution *a priori*. However, there are many cases in which that information is not available, and our chosen form of inductive bias might not fit the underlying distribution very well.

Ideally, we would like to make as few assumptions about the distribution as possible. For example, we can construct a free-form PDF using a piecewise-constant function, in which our model specifies the values of the function over a set of discrete bins. While this is technically still a parametric function, it affords a great deal of flexibility. So much so, in fact, that it performs poorly in many circumstances (as we will show later). However, if each bin has many training samples to draw from, then the law of large numbers should yield a piecewise-constant function that faithfully reflects the underlying true distribution. Unfortunately, the realities of dataset sizes falls far short of that ideal, especially when we use many narrow bins [3].

The shortage of data in each bin can be mitigated in two ways: (1) by applying a smoothness constraint, or (2) by augmenting the data with synthetic but reasonable samples. To address point (1), deconvolution [4] (including forms of convolution with upsampling [5]) is a natural way to encourage smoothness because of its built-in spatial correlation properties. This has the advantage of constructing the PDF in a multiscaled, hierarchical manner through multiple deconvolution layers, allowing the model to introduce structure and smoothness at different scales. To address point (2), we can use a Variational Information Bottleneck (VIB) [6], restricting the latent-space representation to avoid over-fitting.

This paper proposes a Deconvolutional Density Network (DDN) to estimate free-form conditional distributions, $p(y|x)$.

Unlike other techniques, DDN combines deconvolution, multiscale discretization of the output, and a variational layer (using the re-parameterization trick) to construct conditional distributions with greater flexibility, and yet avoid overfitting.

2 Related Work

Conditional density estimation (CDE) has received much attention [1, 7] for its ability to estimate the full distribution rather than just summary statistics, especially when there is uncertainty in the data. In this section, we review previous work in CDE, and describe our motivations for our methods.

Perhaps one of the best-known non-neural CDE methods is the kernel density estimator (KDE) [7]. While simple to use, the KDE suffers from the curse of dimensionality. The kernel quantile regression (KQR) method can predict the percentiles of the conditional distribution [8–10]. One of the downsides of KQR is that it is limited to 1D output. In addition, converting the conditional cumulative distribution to the conditional density requires some heuristic steps, which may result in additional estimation errors. A straightforward CDE method, least-squares conditional density estimation (LSCDE), was proposed by Sugiyama et al. [11], employing the squared loss function.

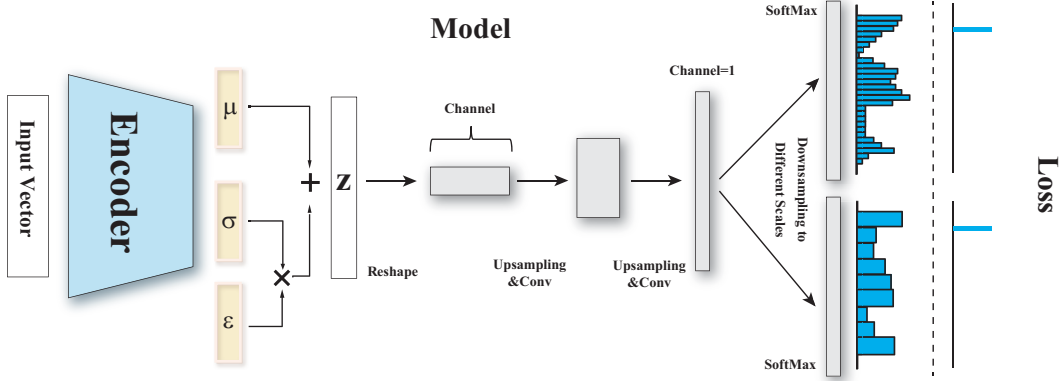


Figure 2: The framework of deconvolutional density network (DDN).

For this method, however, finding an optimal combination of non-negative linear basis functions is very challenging.

Neural networks have been used for CDE for years because of their expressive power. Perhaps the most famous framework is the mixture density network (MDN) [1], which models the conditional density as a mixture of distributions, employing neural networks to predict the parameters of the individual distributions (e.g. mean and standard deviation of a Gaussian). Normalising flows (NFN) [2, 12, 13] are a flexible and efficient approach for fitting complex densities, and provides the PDF in a tractable form. Ambrogioni et al. [14] proposed the kernel mixture network (KMN), combining non-parametric and parametric elements by formulating the CDE model as a linear combination of a family of kernels. On the basis of score matching, Sasaki and Hyvärinen [15] designed a neural-kernelized conditional density estimator (NKC) to estimate the conditional density. A neural noise-regularization and data-normalization scheme for CDE was used for financial applications, addressing problems like overfitting, weight initialization, and hyperparameter sensitivity [16]. Variational methods [17, 18] are another way to approach CDE.

Although theoretically the MDN and NFN methods can approximate any type of distribution, it is still very hard to precisely fit a target distribution if its form is far from the basis functions being used (e.g. Gaussians, or Radial Flows). Therefore, another flexible approach is to transform the CDE task to a discrete domain. A multiscale network transforming the CDE regression task into a hierarchical classification task was proposed in [19] by decomposing the density into a series of half-spaces and learning Boolean probabilities for each split.

Recently, Li et al. [3] described a conditional distribution technique based on deep distribution regression. This method redefines the problem as K binary classification tasks. Although the output nodes are spatially ordered (to form the bins of a distribution), the method ignores the spatial information in previous hidden layers, resulting in distributions that can be very non-smooth.

Using a piecewise-constant function to discretize the continuous-domain distribution has the potential to approximate a free-form conditional distribution, as long as we have sufficiently narrow bins, and enough data. But the strain between infinite-dimensional distributions and finite datasets makes it difficult to faithfully estimate the distribution in real scenarios. However, assuming the true PDFs are commonly smooth and have few spikes, we can use multi-layer deconvolution to construct distributions that exhibit spatial coherence at multiple scales. Furthermore, the re-parameterization trick, shown to be effective for calibrating classifiers [6], could also mitigate the data-shortfall problem faced by piecewise-constant function discretization. In the next section, we describe how our Deconvolutional Density Network (DDN) can infer free-form density functions.

3 Methodology

The complete framework of the proposed Deconvolutional Density Network (DDN) is shown in Fig. 2. The DDN consists of four successive parts: an encoder for mapping the inputs to a latent

space, a variational layer with optional stochasticity, a multi-layer deconvolutional estimator for hierarchical topological smoothness, followed by a partition layer for generating the multiscaled output. By combining these four modules into a single framework, the DDN is able to flexibly estimate conditional density functions.

3.1 Baseline Model

Here we briefly describe the baseline model that is common to all the methods we are comparing. Given an input x , let $f(x, \theta)$ represent a neural network (NN) model, where θ represents all its connection weights and biases. The output of the NN can then be used to generate a continuous-domain function, $g(y; f(x, \theta))$. That is, given a model f , and an input x , the PDF $g : \mathcal{D} \rightarrow \mathbb{R}$ is the probability density of observing y .

If we are given a set of M input/output samples (x_m, y_m) , then the likelihood of observing those samples under our model is,

$$\prod_{m=1}^M g(y_m; f(x_m, \theta)).$$

Taking the log of that likelihood, and negating it, yields the negative log-likelihood,

$$-\sum_{m=1}^M \log g(y_m; f(x_m, \theta)).$$

Our NN model can be trained by attempting to minimize the expected negative log-likelihood of the training data,

$$\arg \min_{\theta} \mathbb{E}_{(x_m, y_m)} [-\log g(y_m; f(x_m, \theta))] = \arg \min_{\theta} \left[-\frac{1}{M} \sum_{m=1}^M \log g(y_m; f(x_m, \theta)) \right]. \quad (1)$$

3.2 Partitioning

In this module, we partition \mathcal{D} , the domain of the variable y , into a number of uniform bins. These bins will be used to construct the CDE as a piecewise-constant function. Discretizing g , we partition the output space into N bins, and denote the i^{th} bin using B_i , with uniform bin width ΔB . If our neural network outputs N values, f_i for $i = 1, \dots, N$, then we simply interpret $f_i(x, \theta)$ as the estimated probability that y falls in the i^{th} bin. Then, the estimated conditional density function can be expressed as a piecewise-constant function,

$$g(y | x) = \begin{cases} \vdots \\ f_i(x, \theta) & \text{if } y \in B_i \\ \vdots \end{cases}.$$

We can write the negative log-likelihood loss function as,

$$\arg \min_{\theta} \left[-\frac{1}{M} \sum_{m=1}^M \log g(y_m | x_m) \right] \quad (2)$$

$$= \arg \min_{\theta} \left[-\frac{1}{M} \sum_{m=1}^M \sum_{i=1}^N \log (f_i(x_m, \theta)) \mathbf{1}_{B_i}(y_m) \right], \quad (3)$$

where $\mathbf{1}_{B_i}(y)$ is an indicator function, equal to 1 when $y \in B_i$, and zero otherwise.

For our DDN, we have found it helpful to output the PDF at a variety of different resolutions. Suppose the network has J different sets of output nodes, where the number of nodes in each set is N_j , corresponding to an N_j -bin partition of the PDF; Fig. 2 shows two such sets of outputs. Then we can include all of these outputs in our loss function, averaging over them all. Thus, our loss function includes a sum over J ,

$$\arg \min_{\theta} \left[-\frac{1}{M} \sum_{m=1}^M \sum_{j=1}^J \sum_{i=1}^{N_j} \log (f_{ij}(x_m, \theta)) \mathbf{1}_{B_{ij}}(y_m) \right], \quad (4)$$

where $f_{ij}(x, \theta)$ is the output of the i^{th} node in the j^{th} set of output nodes, and $\mathbf{1}_{B_{ij}}(y)$ is the indicator variable that equals 1 when $y \in B_{ij}$, and zero otherwise.

3.3 Encoder-Estimator Framework

How does the DDN model avoid the problem of overtraining on insufficient data? In order to avoid over-fitting, and to calibrate the estimated distribution [20], we wish to construct a latent representation that is focused on the statistically salient features of our dataset, not the contingencies specific to our particular training samples. Furthermore, adding randomness into the latent space could help to augment our dataset [20].

We split our network into two main parts: an encoder $q(z|x)$, and an estimator $h(y|z)$; a latent space sits between the two. The encoder outputs two equal-sized vectors, μ and σ , representing the mean and standard deviation for a multi-variate, diagonal Gaussian distribution. Inspired by the variational autoencoder [21], our latent vectors z are stochastic, drawn from that Gaussian distribution using the reparameterization trick, $z = \mu + \sigma \cdot \epsilon$, where ϵ is drawn from the standard Normal distribution, $\epsilon \sim \mathcal{N}(0, I)$. As conventional, we call this latent-space layer a *variational layer* (VL). This reparameterization trick makes the loss function differentiable with respect to μ and σ , thus enabling gradient-based learning of the network parameters that compute μ and σ .

According to VIB [6], it is important to introduce a KL divergence term to the loss function to limit the mutual information between the input and the latent representation. This constraint forces the network to sacrifice some encoding fidelity in order to seek a less complex and more economical latent representation. It encourages the distribution of latent vectors to resemble a standard Normal distribution, $\mathcal{N}(0, I)$. Thus, if $q(z|x) \sim \mathcal{N}(\mu(x; \theta), \sigma^2(x; \theta))$, then we add the term

$$\beta D_{\text{KL}}[q(z|x) \parallel \mathcal{N}(0, I)] \quad (5)$$

to our loss function. The β coefficient controls the flow of information through the latent space [6, 22]. When $\beta = 0$, the latent-space distribution can relax, and spread out, allowing the samples to disambiguate from each other. Increasing β encourages the latent-space distribution to contract toward the origin [6]. In this way, β influences the calibrating estimated distribution [20] by forcing the model to focus on the statistically salient features of the inputs, and thereby help to avoid overfitting.

The final objective function for our proposed DDN method comes from combining (4) and (5),

$$L = \frac{1}{M} \sum_{m=1}^M \left[E_{\epsilon \sim \mathcal{N}(0, I)} \left\{ - \sum_{j=1}^J \sum_{i=1}^{N_j} \log(h_{ij}(y_m|z)) \mathbf{1}_{B_{ij}}(y_m) \right\} + \beta D_{\text{KL}}[q(z|x_m) \parallel \mathcal{N}(0, I)] \right] \quad (6)$$

Recall that h_{ij} and q are both functions of the network parameters, θ . Note that during testing, ϵ is set to 0 to remove latent-space stochasticity.

3.4 Deconvolutional Estimator

Despite its potential to approximate a free-form conditional distribution, discretizing the continuous-domain distribution by a piecewise-constant function often suffers from statistical undersampling in its bins, resulting in a distribution that is very spiky. If we can assume that the true PDFs are commonly smooth and have few spikes, we could include a mechanism that correlates nearby outputs.

In this work, a multi-layer deconvolutional estimator h is designed to instill spatial coherence at different scales. Note that our deconvolutional layers are not there to invert or undo a convolutional layer. Instead, the deconvolutional layers [4] (also known as transposed convolution or upsampling convolution [5]) are used to build the output layer-by-layer, in progressively higher resolution.

In our deconvolutional estimator h , the latent vector z is first reshaped into a multi-channel feature map. The reshaped latent vector is then fed into a sequence of deconvolution layers, constructed from conventional techniques like upsampling and convolution. Upsampling expands the feature map by an integer scale factor, while the convolution transforms the expanded feature map with shared weights introducing spatial correlation. After these deconvolution layers, we obtain a vector of unnormalized logits. This unnormalized logits vector is then downsampled to form J different output layers, each with a different resolution. A SoftMax function is applied to each output layer. At this point, we have J discretized probability vectors. These outputs are used in the loss function (6). Note that we only use the output layer with the highest resolution during testing.

Table 1: Characteristics of datasets from real-world problems.

	Yacht	Boston	Concrete	Fish	Energy	Music
No. of samples	308	506	1030	908	768	1059
No. of features	6	13	8	6	8	68
No. of targets	1	1	1	1	2	2

4 Experiments

4.1 Configuration

Datasets: We used two artificial 1D toy tasks for comparing different models, since we know their ground truth conditional distributions, $p(y|x)$. The tasks are:

M2U: Mixed distribution of two Uniform distributions: $y = ab + (1 - a)c$ where $x \sim U(-1, 1)$, $a \sim \text{Bern}(0.5)$, $b \sim U(-5 + x, -1 + x)$, $c \sim U(1 - x, 5 - x)$

MNG: Mixed distribution of Normal and Gamma distributions: $y = ab + (1 - a)(c + 1 - x)$ where $x \sim U(-1, 1)$, $a \sim \text{Bern}(0.7)$, $b \sim \mathcal{N}(-1 + x, 1 + 0.2x)$, $c \sim \text{Gamma}(1, 1)$

We also adopt six small real-world datasets for verification, including 4 univariate and 2 bivariate tasks. All of the problems were selected from the UCI machine learning repository [23]. All the inputs were standardized by Z-score normalization. Table 1 summarizes the characteristics of these datasets.

Models: We conducted experiments to compare three other neural-network-based CDE methods, including Mixture Density Network (MDN) [1], Normalizing Flows Network (NFN) [2], and Joint Binary Cross Entropy Neural Network (JBCENN) [3]. For fair comparison, we added a nonlinear variational layer to each model, so each model had two parts: an encoder with a variational layer, and a density estimator.

In the toy and univariate tasks, the encoding part consisted of a fully-connected layer with 100 neurons, and a variational layer with 64 latent nodes. The estimator of our DDN contained two Upsample-Conv1D-BatchNorm-LeakyReLU blocks, and one Upsample-Conv1D block. After several upsampling and convolution operations, the number of bins in our DDN was 1024.

To implement multiscaling, we generated eight sets of outputs, downsampling using average pooling, without introducing any new trainable parameters. For MDN, the estimator consisted of 20 Gaussian kernels parameterized by a fully-connected layer. We used the same flow model as [2], which had one affine flow and five radial flows, and an additional fully-connected layer to parameterize them. The estimator of JBCENN was a fully-connected layer with 1024 neurons, so the JBCENN had the same number of bins as our DDN. All the fully connected layers were activated using Leaky ReLU activation with a 0.2 negative slope.

For the bivariate tasks, we replaced the 1D convolution, upsampling, and pooling operations with the corresponding 2D functions for our DDN. Furthermore, we followed the same framework of NFN as [2] to deal with bivariate tasks.

Evaluation Metrics: For the toy tasks, the ground truth conditional probability distribution was known, so we calculated the sum of squared errors (SSE) between the true distribution and the predicted distribution.

Since we did not know the true distributions for the real-world datasets, we had to assess the quality of our estimated distributions using test datasets.

The log-likelihood (LL) measures how probable a set of observations is under a given model. Thus, given set of test samples, we can use the LL to evaluate a CDE model. However, the LL measure is subject to sampling error, so an insufficient test set might not faithfully reflect the quality of the model. Therefore, for univariate problems, we also used the calibration error for regression [24], which measures the reliability of a CDE model by calculating the difference between the model and the empirical frequency from the test data. Let $F_{x_m}(y)$ represent the cumulative probability density of the random variable y given x_m , and set K confidence-level thresholds $0 \leq p_1 \leq p_2 \leq \dots \leq p_K \leq 1$.

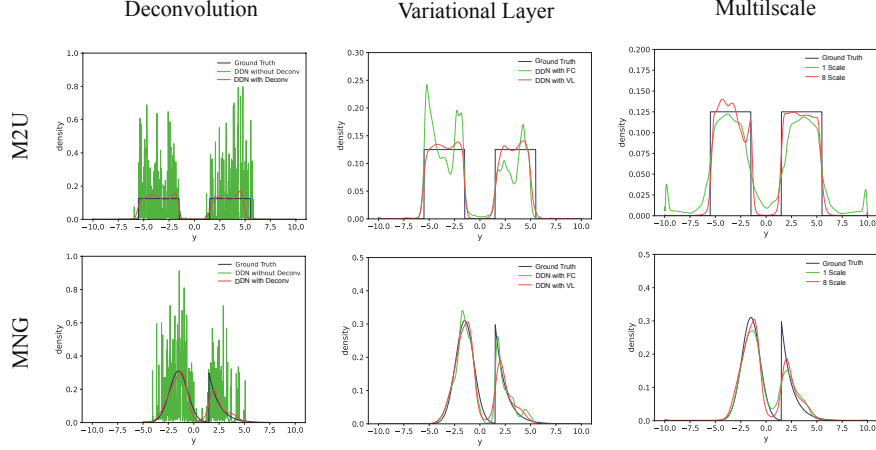


Figure 3: Ablation experiments on two toy problems by removing each of the model’s three main components: deconvolution/fully-connected estimator (first column), variational layer (second column), and single/multiscale output (third column).

For each threshold p_k , we can compute the empirical frequency

$$\hat{p}_k = \frac{|\{y_m | F_{x_m}(y_m) \leq p_k, m = 1, \dots, M\}|}{M}. \quad (7)$$

Then the calibration error is defined as

$$\text{err}(F_{x_1}, y_1, \dots, F_{x_m}, y_m) = \sum_{k=1}^K (p_k - \hat{p}_k)^2. \quad (8)$$

4.2 Ablation Experiment

We have focused our attention on the three components we added to our DDN model: deconvolution, variational layer, and multiscale output. In this section, we systematically remove (ablate) each of the three components to ascertain its influence on the overall performance of the DDN.

To test the effect of using deconvolution in our estimator network, we trained a DDN model with an estimator composed of multiple deconvolution layers, and compared it to a DDN model with an estimator network composed of fully-connected layers.

To test the effect of the variational layer, we trained two versions of our DDN, one with a variational layer (including adding noise to the latent space, and a KL divergence loss term), and one in which the variational layer is replaced by a fully-connected layer with the same number of nodes.

Finally, to test the effect of multiscaled output, we trained a DDN with only one output resolution of 1024 bins, and compared it to a DDN trained with 8 different outputs of differing resolutions (containing 1024, 512, 256, 128, 64, 32, 16, and 8 nodes).

We trained and tested all 6 of those models on each of the toy datasets (M2U, and MNG). The results are shown in Fig. 3. For each of the three features, removing the feature had a negative effect on the model’s performance. The difference was smaller for the number of output scales. However, the effect of removing the variational layer was larger, and the impact of using a fully-connected estimator network (instead of a deconvolution network) was profound. These experiments show that each of the three components in the DDN model contributes something to the performance of the overall system.

4.3 Performance

Toy Tasks: For each toy task, we randomly generated 500 samples for training, and 20,000 samples for testing. We calculated the test SSE between the true distribution and the model’s estimated distribution, and averaged over ten independent trials. The results are illustrated in Fig. 4.

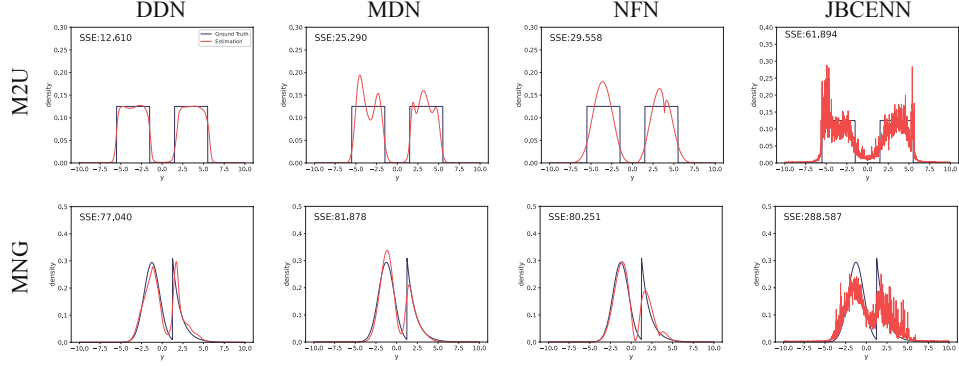


Figure 4: Comparison of estimated density curves and SSE by DDN, MDN, NFN, and JBCENN on toy problems for a specific x . We used 20,000 samples to calculate the average SSE between the ground truth and estimated probability density over ten independent trials.

Table 2: Comparison of calibration error on real-world tasks over 10 independent trials. The mean and standard deviation is given for the different methods. Lower is better.

Dataset	MDN	NFN	JBCENN	DDN
Yacht	1.131±0.472	1.229±0.886	0.549±0.395	0.377±0.328
Yacht (30% uniform noise)	0.806±0.297	0.424±0.445	0.550±0.449	0.168±0.082
Boston	1.163±0.658	0.858±0.838	0.511±0.243	0.332±0.266
Boston (30% uniform noise)	1.443±0.476	0.543±0.390	0.676±0.249	0.240±0.281
Concrete	0.616±0.324	0.422±0.299	0.302±0.144	0.106±0.091
Concrete (30% uniform noise)	0.562±0.173	0.452±0.227	0.295±0.132	0.136±0.117
Fish	0.612±0.280	0.550±0.421	0.515±0.466	0.223±0.126
Fish (30% uniform noise)	0.602±0.261	0.500±0.273	0.331±0.257	0.164±0.127

Our DDN achieves the best performance on the two toy tasks. Although the MDN and NFN methods could fit the Gaussian peak in the MNG task, they fail to fit the uniform distributions in the M2U task, and the Gamma distribution in the MNG task. Notice that JBCENN, which is also a partitioning method (but does not use deconvolution), exhibits many spikes, indicating that deconvolution is an important part of constructing a smooth distribution.

Univariate Real-World Tasks: We trained each model on the univariate datasets 10 times independently. For each trial, we randomly split the data into a training set and test set with a ratio of 8:2. The critical hyperparameter β , which governs the weight of the KL divergence loss term, was chosen by minimizing the calibration error over a grid search on the training set. The statistics of calibration error and log-likelihood over the 10 trials are reported.

Furthermore, to test the flexibility of the models, we created a second version of the real-world datasets with increased uncertainty. We added uniform noise to the original normalized inputs using $x'_m = (1 - \alpha)x_m + \alpha U(-1, 1)$, where α is set to 30%. During testing, for each test sample x_m , we generated 100 random variants x'_m .

Table 2 and Table 3 list the results. The DDN outperforms all competitors on calibration error, and also outperforms most competitors on log-likelihood. The DDN’s ability to model free-form distributions makes it insensitive to the increased uncertainty introduced by the noise; the other methods suffer with the increased uncertainty.

Bivariate Real-World Tasks: We compared MDN, NFN and DDN on two bivariate datasets. We used the same training/testing data split as the univariate tasks, and used trial-and-error to find the best β for each model. We repeated the experiment 10 times for each model.

Table 3: Comparison of log-likelihood on real-world tasks. The mean and standard deviation is given for the different methods. Higher is better.

Dataset	MDN	NFN	JBCENN	DDN
Yacht	-0.718±0.592	-0.155±0.265	-8.431±0.438	-2.051±0.801
Yacht (30% uniform noise)	-4.037±0.529	-1.993±0.281	-12.634±1.105	-2.108±0.169
Boston	-3.762±0.697	-2.677±0.276	-9.292±0.610	-2.550±0.185
Boston (30% uniform noise)	-4.425±0.613	-3.057±0.409	-7.547±0.500	-2.686±0.124
Concrete	-3.376±0.285	-3.119±0.140	-4.256±0.017	-3.246±0.090
Concrete (30% uniform noise)	-4.137±0.191	-3.714±0.070	-4.259±0.013	-3.639±0.065
Fish	-2.049±0.185	-1.467±0.134	-2.361±0.129	-1.347±0.081
Fish (30% uniform noise)	-2.122±0.278	-1.531±0.134	-2.427±0.245	-1.372±0.060

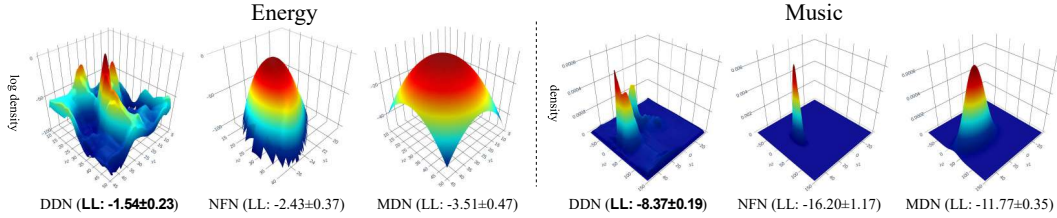


Figure 5: Estimated conditional distributions for a specific x using DDN, NFN, and MDN for bivariate tasks. Note that the vertical axis for the Energy task uses a logarithmic scale.

Figure 5 shows the results. Our DDN yields the best log-likelihood among all the methods. Furthermore, the distributions generated by the DDN illustrate its flexibility in constructing a complicated density function.

5 Conclusion

Our proposed Deconvolutional Density Network (DDN) compares favourably against competing methods at generating conditional distributions that match the true distributions of the datasets. This capability was demonstrated both on toy datasets, for which the true data distributions were known, as well as on real-world datasets, in which the performance of the CDE methods were assessed based on a test set. In the toy datasets, the DDN model clearly outperformed the other methods. In the real-world datasets, the DDN method was not always the best method on all datasets, but it showed the best all-around performance. This was especially true for the noisier versions of those datasets.

A set of ablation experiments showed that each of the three main components of the DDN contributes to the model’s performance; removing any one of the three components resulted in a drop in performance. The drop was especially profound when the estimator network was composed of fully-connected layers, rather than deconvolutional layers. This result is why we chose to put the word "Deconvolutional" in the name of our method.

Much more work remains to fully unpack the features and limitations of the DDN. For example, how does the deconvolution architecture (number of layers, kernel size) affect the performance? How does the dimension of the latent space depend on the dataset? Is there a better alternative to using piecewise-constant functions for creating our free-form distributions?

References

- [1] C. M. Bishop. Mixture density networks. *NCRG/94/004*, 1994. URL <https://ci.nii.ac.jp/naid/10012741982/en/>.
- [2] Brian L Trippe and Richard E Turner. Conditional Density Estimation with Bayesian Normalising Flows. *arXiv e-prints*, art. arXiv:1802.04908, February 2018.
- [3] Rui Li, Brian J. Reich, and Howard D. Bondell. Deep distribution regression. *Computational Statistics & Data Analysis*, 159:107203, 2021. ISSN 0167-9473. doi: <https://doi.org/10.1016/j.csda.2021.107203>. URL <https://www.sciencedirect.com/science/article/pii/S0167947321000372>.
- [4] Yang Yu, Zhiqiang Gong, Ping Zhong, and Jiaxin Shan. Unsupervised representation learning with deep convolutional neural network for remote sensing images. In Yao Zhao, Xiangwei Kong, and David Taubman, editors, *Image and Graphics*, pages 97–108, Cham, 2017. Springer International Publishing. ISBN 978-3-319-71589-6.
- [5] E. Shelhamer, J. Long, and T. Darrell. Fully convolutional networks for semantic segmentation. *IEEE Transactions on Pattern Analysis & Machine Intelligence*, 39(04):640–651, apr 2017. ISSN 1939-3539. doi: 10.1109/TPAMI.2016.2572683.
- [6] Alexander A. Alemi, Ian Fischer, Joshua V. Dillon, and Kevin Murphy. Deep variational information bottleneck. *5th International Conference on Learning Representations, ICLR 2017 - Conference Track Proceedings*, pages 1–19, 2017.
- [7] Alexandre B. Tsybakov. *Introduction to Nonparametric Estimation*. Springer Publishing Company, Incorporated, 1st edition, 2008. ISBN 0387790519.
- [8] Ichiro Takeuchi, Quoc V. Le, Timothy D. Sears, and Alexander J. Smola. Nonparametric quantile estimation. *Journal of Machine Learning Research*, 7(45):1231–1264, 2006. URL <http://jmlr.org/papers/v7/takeuchi06a.html>.
- [9] Youjuan Li, Yufeng Liu, and Ji Zhu. Quantile regression in reproducing kernel hilbert spaces. *Journal of the American Statistical Association*, 102(477):255–268, 2007. doi: 10.1198/016214506000000979. URL <https://doi.org/10.1198/016214506000000979>.
- [10] Ichiro Takeuchi, Kaname Nomura, and Takafumi Kanamori. Nonparametric Conditional Density Estimation Using Piecewise-Linear Solution Path of Kernel Quantile Regression. *Neural Computation*, 21(2):533–559, 02 2009. ISSN 0899-7667. doi: 10.1162/neco.2008.10-07-628. URL <https://doi.org/10.1162/neco.2008.10-07-628>.
- [11] Masashi Sugiyama, Ichiro Takeuchi, Taiji Suzuki, Takafumi Kanamori, Hirotaka Hachiya, and Daisuke Okanohara. Least-Squares Conditional Density Estimation. *IEICE Transactions on Information and Systems*, 93(3):583–594, January 2010. doi: 10.1587/transinf.E93.D.583.
- [12] Danilo Rezende and Shakir Mohamed. Variational inference with normalizing flows. In Francis Bach and David Blei, editors, *Proceedings of the 32nd International Conference on Machine Learning*, volume 37 of *Proceedings of Machine Learning Research*, pages 1530–1538, Lille, France, 07–09 Jul 2015. PMLR. URL <http://proceedings.mlr.press/v37/rezende15.html>.
- [13] Laurent Dinh, Jascha Sohl-Dickstein, and Samy Bengio. Density estimation using real NVP. 2017. URL <https://arxiv.org/abs/1605.08803>.
- [14] L. Ambrogioni, Umut Güçlü, M. V. Gerven, and E. Maris. The kernel mixture network: A nonparametric method for conditional density estimation of continuous random variables. *arXiv: Machine Learning*, 2017.
- [15] Hiroaki Sasaki and Aapo Hyvärinen. Neural-kernelized conditional density estimation, 2018.
- [16] Jonas Rothfuss, Fabio Ferreira, Simon Walther, and Maxim Ulrich. Conditional Density Estimation with Neural Networks: Best Practices and Benchmarks. Papers 1903.00954, arXiv.org, March 2019. URL <https://ideas.repec.org/p/arx/papers/1903.00954.html>.
- [17] Charlie Tang and Russ R Salakhutdinov. Learning stochastic feedforward neural networks. In C. J. C. Burges, L. Bottou, M. Welling, Z. Ghahramani, and K. Q. Weinberger, editors, *Advances in Neural Information Processing Systems*, volume 26. Curran Associates, Inc., 2013. URL <https://proceedings.neurips.cc/paper/2013/file/d81f9c1be2e08964bf9f24b15f0e4900-Paper.pdf>.

- [18] Kihyuk Sohn, Honglak Lee, and Xinchen Yan. Learning structured output representation using deep conditional generative models. In C. Cortes, N. Lawrence, D. Lee, M. Sugiyama, and R. Garnett, editors, *Advances in Neural Information Processing Systems*, volume 28. Curran Associates, Inc., 2015. URL <https://proceedings.neurips.cc/paper/2015/file/8d55a249e6baa5c06772297520da2051-Paper.pdf>.
- [19] Wesley Tansey, Karl Pichotta, and James G. Scott. Better Conditional Density Estimation for Neural Networks. *arXiv e-prints*, art. arXiv:1606.02321, June 2016.
- [20] Alexander A. Alemi, Ian Fischer, and Joshua V. Dillon. Uncertainty in the Variational Information Bottleneck. *arXiv e-prints*, art. arXiv:1807.00906, July 2018.
- [21] Diederik P. Kingma and Max Welling. An introduction to variational autoencoders. *Foundations and Trends in Machine Learning*, 12(4):307–392, 2019. ISSN 1935-8245. doi: 10.1561/22000000056. URL <http://dx.doi.org/10.1561/22000000056>.
- [22] I. Higgins, Loïc Matthey, A. Pal, Christopher P. Burgess, Xavier Glorot, M. Botvinick, S. Mohamed, and Alexander Lerchner. beta-VAE: Learning basic visual concepts with a constrained variational framework. In *ICLR*, 2017.
- [23] Dheeru Dua and Casey Graff. UCI machine learning repository, 2017. URL <http://archive.ics.uci.edu/ml>.
- [24] Volodymyr Kuleshov, Nathan Fenner, and Stefano Ermon. Accurate uncertainties for deep learning using calibrated regression. In Jennifer Dy and Andreas Krause, editors, *Proceedings of the 35th International Conference on Machine Learning*, volume 80 of *Proceedings of Machine Learning Research*, pages 2796–2804. PMLR, 10–15 Jul 2018. URL <http://proceedings.mlr.press/v80/kuleshov18a.html>.